2021

Polystyrene Microplastics Reduce Abundance Of Developing B Cells In Rainbow Trout (Oncorhynchus mykiss) Primary Cultures

Patty Zwollo
William & Mary - Department of Biology

Fatima Quddos
William & Mary - Department of Biology

Carey Bagdassarian
William & Mary - Interdiscipliinary Studies

Meredith Evans Seeley
Virginia Institute of Marine Science

Robert Hale
Virginia Institute of Marine Science

See next page for additional authors

Follow this and additional works at: https://scholarworks.wm.edu/vimsarticles

Part of the Immunology and Infectious Disease Commons

Recommended Citation

Authors

Patty Zwollo, Fatima Quddos, Carey Bagdassarian, Meredith Evans Seeley, Robert Hale, and Lauren Abderhalden

1

2

3

Polystyrene Microplastics Reduce Abundance Of Developing B Cells

In Rainbow Trout (*Oncorhynchus Mykiss*) Primary Cultures.

6

7

Patty Zwollo[1][¶], Fatima Quddos[1], Carey Bagdassarian[2], Meredith Evans Seeley[3], Robert C.

Hale[3], and Lauren Abderhalden[1]

[1]Department of Biology, William and Mary, Williamsburg, VA 23185.

[2]Interdisciplinary Studies, William and Mary, Williamsburg, VA 23185

[3]Virginia Institute of Marine Science, Department of Aquatic Health Sciences, William & Mary,

Gloucester Point, VA 23062

15

16

17

¶ Corresponding author

Patty Zwollo

Department of Biology

William and Mary

Williamsburg, VA 23185

FAX: 757-221-6483

Phone: 757-221-1969

pxzwol@wm.edu

26 **ABSTRACT**

27   Environmental microplastic pollution (including polystyrene, PS) may have detrimental

28 effects on the health of aquatic organisms. Accumulation of PS microplastics has been reported

29 to affect innate immune cells and inflammatory responses in fish. To date, knowledge on effects

30 of microplastics on the antibody response is still very limited. Here, we investigated effects of

31 small (0.8-20 µm) PS microplastics on the abundance of B lineage cells in primary cultures of

32 developing immune cells from the anterior kidney of rainbow trout. Both purchased PS

33 microbeads and PS microparticles generated from consumer products were used as

34 microplastic sources. We first show that rainbow trout phagocytic B cells efficiently took up small

35 (0.83-3.1µm) PS microbeads within hours of exposure. In addition, our data revealed that PS

36 microplastic exposure most significantly decreased the abundance of a population of non-

37 phagocytic developing B cells, using both flow cytometry and RT-qPCR. PS microplastics-

38 induced loss of developing B cells further correlated with reduced gene expression of RAG1 and

39 the membrane form of immunoglobulin heavy chains mu and tau. Based on the induced loss of

40 developing B cells observed in our *in vitro* studies, we speculate that *in vivo*, chronic PS

41 microplastic-exposure may lead to suboptimal IgM/IgT levels in response to pathogens in

42 teleost species. Considering the highly conserved nature of vertebrate B lymphopoiesis it is

43 likely that PS microplastics will similarly reduce antibody responses in higher vertebrate species,

44 including humans. Further, RAG1 provides an effective biomarker to determine effects of PS

45 microplastics on B cell development in teleost species.

46

47

48

49

50

51

INTRODUCTION

The rapid global increase in plastic use and production has led to accumulation of plastic debris in the natural environment (Jambeck et al., 2015; Borrelle et al. 2017). Plastic pollution has been documented across nearly all natural environments, with extensive research emphasis on its distribution in and impact upon freshwater and marine ecosystems (Hale et al., 2020). This debris is abrased and weathered over time in the environment, forming fragments including microplastics (1 µm – 5 mm diameter; Hartmann et al. 2019). These 'secondary microplastics' are far more abundant than manufactured 'primary' microplastic particles (Hartmann et al., 2019; Hale et al. 2020). As the majority of plastic debris derives from single-use products, microplastic pollution is dominated by polymers therein, including polyethylene, polypropylene and polystyrene (PS) (Geyer et al. 2017; Borrelle et al. 2017). The potential impacts of these microplastics on aquatic resources have been explored, with particular emphasis on PS microplastics as they are more easily purchased as spherical microbeads in the micro and nanoplastic size range than other polymers. Accumulation of PS microplastics has been observed in fish intestines, gills and skin (Choi et al., 2018; Zitouni et al., 2020; Espinosa et al., 2018). Besides acute mortality, some exposure studies suggest that more complex impacts, including immune function, merit further investigation (Bucci et al. 2019).

Most studies investigating the immune response to microplastics in fish have focused on innate immunity, and generally suggest that microplastic exposure has an activating role. In one study, injection of zebrafish (*Danio rerio*) larvae with 0.7 µm PS microbeads enhanced expression of complement genes and, further, led to co-localization of PS microplastics and neutrophils/macrophages (Veneman et al., 2017). Limonta et al. (2019) found increased abundance of neutrophils in gills and intestinal epithelium of zebrafish after exposure to PS microbeads and enhanced expression of Major Histo Compatibiity (MHC) Class II genes. Greven et al. (2016) noted increased neutrophil degranulation and extracellular trap release in fathead minnow (*Pimephales promelas*) after exposure to 41 nm sized PS microbeads. Hamed

78   et al. (2019) noticed a significant decline in monocytes in the blood of juvenile Nile tilapia

79   (*Oreochromis niloticus*) after a 15-day exposure to irregularly-shaped PS microbeads (>0.1 µm)

80   at concentrations of 1, 10, 100 µg/ml.

81   Microplastics may also have significant effects on cytokine production in teleost species. For

82   example, increased overall expression of pro-inflammatory Interleukin-1β (IL1β) was noted 24

83   hours after injection of 0.25 nm sized PS nanoplastics in zebrafish embryos, and similarly after

84   waterborne exposure (Brun et al., 2018). However, Lu et al. (2018) found that expression

85   of *il1β* genes was downregulated in rainbow trout gills after 2 hours of exposure to 1 µm sized

86   PS microplastics. Size of PS microplastic, exposure period, and/or the target tissue likely affect

87   the IL1β response pathway differentially. Lu et al. (2018) observed significant upregulation of

88   the type II interferon-γ (*ifnγ)* gene in rainbow trout gills after exposure to 0.2 µm and 40 µm sized

89   PS microbeads, and in zebrafish exposed to 1 µm and 90 µm sized PS microbeads. Zebrafish

90   exposed to 0.2 and 20 µm sized PS microbeads down-regulate expression of the *il8* gene (Lu et

91   al 2018). Together, studies so far suggest that PS microplastics have significant dysregulating

92   and/or pro-inflammatory effects on the innate immune system of teleosts.

93   Phagocytosis may be an important pathway for the uptake of microplastics by immune

94   cells. Teleost myeloid lineage professional phagocytes, such as macrophages and neutrophils,

95   can rapidly phagocytose particles smaller than themselves, generally < 10 µm in diameter with

96   maximum efficiency between 3-5 µm (Champion et al. 2008). Further, teleost B cells exhibit

97   phagocytic properties; in rainbow trout (*Oncorhynchus* mykiss) B cells were able to engulf 0.5 to

98   2 µm sized PS particles *in vivo* and *in vitro* (Li et al., 2006). However, fewer studies have

99   focused on this aspect of immunity in response to microplastic pollution.

100   Despite extensive research on the innate immune system, very little is known about effects

101   of PS microplastics on B-cell development. In teleost fishes, immune cells are generated in the

102   anterior kidney through B lymphopoiesis. Various B lineage cell populations at this

103   hematopoietic site have been defined by flow cytometric and quantitative polymerase chain

104   reaction (qPCR) analyses (Zwollo, 2011; Moore et al., 2019). Developing B cells co-express B-

105   cell specific transcription factor Pax5 and Recombination Activating Gene-1 (RAG1; Zwollo et

106   al., 2010), but have low expression of the membrane-bound form of immunoglobulin (Ig) mu

107   (IgM) or tau (IgT; Zwollo et al., 2008; Zwollo et al., 2017). In contrast, immature and mature B

108   cells co-express Pax5 and membrane-bound IgM or IgT, but not RAG1 (Zwollo et al., 2008;

109   Zwollo et al, 2017). IgM is the most prevalent systemic Ig, while IgT plays essential roles in

110   mucosal immunity and microbiota homeostasis (Hansen et al., 2005) (Salinas et al., 2011) (Xu

111   et al., 2020). A third isotype, IgD, is expressed at relatively low concentrations and is involved in

112   mucosal homeostasis (Perdiguero et 2019). Our group has also reported on an early

113   developing B cell population which co-expresses Pax5, IL1β, and a marker recognized by the

114   myeloid/granulocyte antibody Q4E (MacMurray et al., 2013; Moore et al., 2019). A summary of

115   these cellular phenotypes based on these markers is listed in Table I.

116   Existing work motivates further research regarding B cell responses to microplastics.

117   Rubio et al. (2020) exposed a human B cell line to 50nm PS microbeads and found

118   compromised cell viability after 24- and 48-hour exposure *in vitro*. A recent report by Gu et al.

119   (2020) found that exposure of zebrafish intestinal cell cultures to PS microbeads induced down-

120   regulation of genes within the immune network for Ig Z/tau production, using single cell RNA-

121   sequencing; this suggests that PS microbeads disrupt the mucosal antibody response. In

122   contrast, exposure to 1 µm PS microbeads *in vivo* resulted in upregulation of the Ig heavy chain

123   mu (HCmu) gene after a short (2-hour) exposure in gills of zebrafish but not rainbow trout (Lu et

124   al., 2018). And, again, B cells have been noted to phagocytize PS microparticles (Li et al.,

125   2006).

126   Here, we investigated *in vitro* effects of small (0.8-20 µm) PS microplastics on B cell

127   populations in anterior kidney cultures of rainbow trout. Two forms of PS microplastics were

128   used: purchased PS microbeads (perfectly spherical particles, commonly used in studies on

129   phagocytosis of immune cells) and PS microparticles generated from consumer products

130   (irregularly shaped, akin to most microplastics in the environment). Hereafter, these will be

131   distinguished as PS microbeads and PS microparticles, respectively, or cumulatively as PS

132   microplastics. Based on published work (Li et al. 2006), we predicted that phagocytic B cells

133   would preferentially take up small PS microplastics (1-2 µm). Further, we hypothesized that the

134   main effects of PS microplastics would be a consequence of phagocytosis, resulting in reduced

135   cell viability and/or apoptosis of B cells. However, our results revealed that PS microplastic

136   exposure most significantly affected a population of Pax5 and RAG1 co-expressing

137   (Pax5^{+}/RAG1^{+}) non-phagocytic developing B cells. This result was further supported by gene

138   expression analyses targeting immune-related genes. Together, our data reveal a dose- and

139   size-dependent *decrease* in developing B cells after exposure to PS microplastics in culture. We

140   propose that this may ultimately result in suboptimal humoral immune responses to pathogens

141   in PS microplastic-exposed fish.

142

143   METHODS

144   **Cell lines**

145   The carp macrophage cell line CLC (European Collection of Cell Cultures # 95070628)

146   was grown according to instructions, as follows: DMEM medium with 2mM Glutamine, 1% non-

147   essential amino acids, 50 µg/ml gentamycin, and 10% heat-inactivated fetal bovine serum

148   (FBS).

149

150   **Rainbow trout cells and primary cultures**

151   Naïve rainbow trout (30-75 grams) were euthanized and white blood cells (wbc) from the

152   anterior kidney isolated by centrifugation through a Histopaque density gradient, as described

153   previously (Zwollo et al., 2008). The cell yield after Histopaque purification was typically

154   between $0.2 – 2 \times 10^7$ cells per fish, providing sufficient purified anterior kidney wbcs for one

155   type of experiment, either flow cytometry or gene expression. Wbcs were cultured in trout

156   culture medium (TCM) in the presence of LPS (*F. psychrophilum* strain CSF259-93) at 50 µg/ml

157   at 10^7 cells/ml at 18˚C and in the presence of blood gas (10% CO_2, 10% O_2, 80% N_2) as

158   described elsewhere (Zwollo et al., 2015), Yui and Kaattari 1987*). Cells were fed after 48 hours

159   with one tenth of the culture volume of a 10x tissue culture cocktail (Zwollo et al., 2008)

160   containing 500 µg/ml gentamycin, 10x essential aas, 10x non-essential aas, 70 mM L-

161   glutamine, 70 mg/ml dextrose, 10x nucleosides, and 33% FBS.

162

163   **Polystyrene microparticles**

164   Biotinylated PS microbeads were purchased from Spherotech Inc. in four sizes: 0.83 µm

165   (range 0.7-0.9 µm), 3.1 µm (range 3.0-3.9 µm), 6.8 µm (range 6.0-8.0 µm), and 16.5 µm (range

166   13.0-17.9 µm). Stock solutions of beads were made to 5 mg/ml in phosphate-buffered saline

167   (PBS; 0.137 M NaCl, 0.0027 M KLC, 0.01 M Na_2HPO_4, and 0.0018 M KH_2PO_4, pH 7.4),

168   containing 0.02% sodium azide (PBSA). 10-fold serial dilutions were made from the stock

169   solutions in sterile PBSA in the range of 0.01-100 µg/ml. PS microbeads were vortexed for 30

170   seconds immediately before adding to cell cultures.

171   For some of the experiments, the total volume of PS microbeads added to each culture

172   was calculated (independent of particle size) considering a PS density of 1.05 g/ml: 0.1 µg/ml of

173   PS beads have a volume of 9.5×10^{-8} cm^3, 1 µg/ml of PS beads have a volume of 9.5×10^{-7}

174   cm^3,10 µg/ml of PS beads have a volume of 9.5×10^{-6} cm^3, and 100 µg/ml pf PS beads have a

175   volume of 9.5×10^{-5} cm^3.

176   Expanded PS packaging material (a common form of single-use containers) was used to

177   create irregularly shaped PS microparticles, generated via cryogenic grinding (Retzch CryoMill)

178   and sieving with a 20 µm tapper sieve, as in Seeley et al., 2020. The resulting material ranged

179   from ~1-40 µm, with 50% of particles being ≤16 µm (size distribution and image: Supplementary

180   Figure 1). The same concentrations were used in these experiments as the purchased PS

181   microbeads experiments. PS particles were serially diluted 10-fold in RPMI1640 medium

182   containing 10% FBS (Thermofisher SCI) to generate single-particle suspensions. A control

183   cocktail of biotinylated PS microbeads was made to mimic the size distribution of the irregularly

184   shaped PS microparticles (Supplementary Figure 1) and contained 0.1% 0.83 µm particles: 4%

185   3.1 µm particles: 28% 6.8 µm size particles, and 68% 16.5 µm particles.

186   For cell line cultures or anterior kidney primary cell cultures, various types and sizes of

187   PS microplastics in concentrations ranging from 0-100 µg/ml were added immediately after

188   plating the cells from 100x stock solutions, followed by gentle resuspension. After incubation

189   with PS microplastics was complete, cells were collected for fixing (see below) or alternatively,

190   cells were spun at 400 g for 10 minutes, cell pellets resuspended in 1 ml RNazol-RT (Molecular

191   Research Center, Inc), and stored at -80˚C until RNA extraction.

192

193   **Antibodies**

194   The monoclonal mouse anti-trout immunoglobulin heavy chain mu (HCmu, or I-14;

195   (DeLuca, 1983) was a gift from Dr. Greg Warr. The monoclonal mouse anti-trout

196   immunoglobulin tau antibody (41.8; (Zhang et al., 2010) recognizes IgT1, IgT2, and IgT3 (Zhang

197   et al., 2017) and was a gift from Dr. Oriol Sunyer. The rabbit polyclonal Pax5 antibody

198   (previously called ED-1; (Zwollo et al., 2008) recognizes the paired domain of vertebrate Pax5

199   and detects trout Pax5 in pre-B through plasmablast stages (MacMurray et al., 2013). The rabbit

200   polyclonal RAG1 antibody (H300; recognizing amino-acids 744-1043 of the human RAG

201   protein) was purchased from Santa Cruz Biotech, and has been used in previous studies

202   (Zwollo, et al 2010). The Q4E monoclonal antibody was a gift from Drs. Kuroda and Dr. Bernd

203   Kollner (Friedrich-Loeffler Institute, Federal Research Institute, Germany), and recognizes

204   rainbow trout granulocytes, monocytes and macrophages, but not resting mature lymphocytes

205   or thrombocytes (Kuroda et al., 2000). Isotype control antibodies included rabbit IgG or mouse

206 IgG (eBiosciences) conjugated to Alexa Fluor 555 or Alexa Fluor 647. All antibodies were

207 aliquoted and stored in 1% BSA at –20°C.

208

209 **Cell collection, fixation, and flow cytometry**

210 Before collecting cells for fixing, images of the cultures in the culture plates were made

211 on a phase-contrast microscope with a LabCam Microscope Adaptor for iPhone 7/8 (iDu

212 Optics). Collected cells were fixed in 1% ice-cold paraformaldehyde (10% stock, EM-grade;

213 Electron Microscopy Sciences) and permeabilized in 1 mL ice-cold 80% methanol, as described

214 previously (Zwollo et al., 2010). After overnight incubation at -20°C, cells were either

215 resuspended in permeabilizing solution (BD perm wash in PBS, BD Biosciences) and stained as

216 described previously, or refixed for long-term storage at -80˚C in FBS containing 10% DMSO

217 (Zwollo et al., 2010; MacMurray 2013). Percentages of cells with phagocytosed particles were

218 monitored using streptavidin-APC750 (1:1500; Thermofisher SCI.) prior to antibody staining.

219 Approximately 30,000 events were acquired per sample using a BD FACSArray (BD

220 Biosciences). Duplicate samples for each staining combo were run for each experiment.

221 Contour graphs were generated using WinMDI 2-8 (J. Trotter 1993–1998) software.

222

223 **Proliferation and cell viability.**

224 Cell proliferation rates were determined using a Click-it kit (Thermofisher SCI.) in

225 combination with antibody staining and followed by flow cytometric analysis, as described

226 previously (Barr et al., 2011). Cell viability was determined using the fixable viability staining kit

227 Live-or-Dye 564/583, following the manufacturer's instructions (Biotium), and was followed by

228 antibody staining and flow cytometric analysis.

229

230 **RNA Extraction, cDNA synthesis, and qPCR.**

231   Total RNA in RNAzol RT (Molecular Research Center, Inc) was purified according to

232   manufacturer's instructions. RNA concentration was measured using a Nanodrop ND-1000

233   Spectrophotometer (Thermofisher SCI.) and RNA stored at -80°C for future use. cDNA was

234   synthesized using iScript™ Reverse Transcriptase Supermix for RT-qPCR, using random

235   primers (Bio-Rad Laboratories, Inc.). Quantitative real-time PCR to determine expression of

236   memHCmu, secHCmu, memHCtau, secHCtau and a-tubulin have been described previously

237   (Chappell et al., 2017; Quddos and Zwollo, 2021). A custom RAG1 Taqman probe was

238   developed by Thermofisher SCI. Forward primer: 5'-GCG CTG CTG GAC ATTGG-3', reverse

239   primer: 5'-GGT CTC CAC CCA GGG ACA T, and reporter 5'-CAG CTT CTC CAG GAC CC-3.

240   All qPCR assays were performed using a StepOne Real-Time PCR instrument (Applied

241   Biosystems Inc). Average CT scores from triplicate samples were determined for each target

242   gene. Fold change (RFC) was determined by subtracting the delta $[CT(target_{ref})\text{-}CT(tubulin_{ref})]$

243   of a control fish from the $delta[CT(target_{sample})\text{-}CT(tubulin_{sample})]$ of each sample to obtain ddCT,

244   and $2^{\wedge}\text{-}ddCT$ calculated for each sample. Relative fold-change was calculated by normalizing

245   the "no bead" values to 100%.

246

247   **RESULTS**

248   **Phagocytosis in a teleost macrophage cell line**

249   Initially, patterns of phagocytosis were investigated using a fish cell line, carp

250   macrophage cell line CLC. Cells were exposed to four sizes of PS microbeads (0.83 µm, 3.1

251   µm, 6.8 µm, and 16.5 µm) under varying particle concentrations (0, 0.01, 0.1, 1, 10, and 100

252   µg/ml). The PS microbeads contained a biotin conjugate to enable intracellular detection using

253   fluorochrome SA-APC750. The smallest size (0.83 µm) was selected because it most closely

254   mimics the size of bacterial particles. The largest size (16.5 µm) was selected to measure

255   effects on cells independent of phagocytosis. PS microbead uptake was measured as early as 2

256   hours after exposure, but uptake was highest after 16 hours, and returned to background levels

257   after 3 days.

258   As expected, cellular exposure to higher concentrations of PS microbeads resulted in a

259   higher percentage of cells that had phagocytosed PS microbeads (Figure 1A). Smaller PS

260   microbeads were taken up more frequently than larger sizes: at 100 µg/ml concentrations of

261   beads, 60.7% +/- 6.6 of the cells (using 0.83 µm size PS), 5.96 % +/- 2.66 of the cells (using 3.1

262   µm PS), 15.2% +/- 1.82% of the cells (for 6.8 µm PS), and 3.48% +/- 1.24% of the cells (for 16.5

263   µm PS.

264   To rule out effects from non-specific binding (e.g., by PS microbeads adhering to the cell

265   surface), a negative control sample was included: CLC cells were combined with 100 µg/ml PS

266   microbeads (for each size) and processed immediately. The percentage of nonspecific binding

267   was not significantly different from the negative controls (not shown), supporting that the

268   measured percentage of APC-750-positive cells reflects the level of phagocytosis in the test

269   samples.

270   Phagocytosis of PS microplastics could potentially be expected to increase cell death,

271   especially based on our observation that phagocytosis-positive cells were lacking after 3 days.

272   However, no significant differences in viability were observed within the time period studied.

273

274   **Phagocytosis by trout immune cells.**

275   To identify immune cell populations that have the ability to phagocytose PS microbeads

276   in fish, purified wbcs from the anterior kidney of rainbow trout were cultured in the presence of

277   biotinylated PS microbeads for either 16 hours or 3 days. The abundance of myeloid cells that

278   had taken up PS microbeads was determined by 2-color flow cytometry using myeloid marker

279   Q4E (Moore et al, 2019), in combination with the SA-APC750 marker, as described for CLC

280   cells.

281   The average abundance of APC750-positive myeloid-lineage cells (APC750$^+$/Q4E$^+$) was

282   higher after 16 hours compared to after 3 days (Figure 1B and Supplemental Figure 2,

283   respectively). After 16 hours of exposure, myeloid cells phagocytosed the smallest PS

284   microbeads most efficiently, and uptake abundance decreased as PS microbead size increased

285   (at 100 µg/ml bead concentration: 8.73% +/- 0.93 for 0.83 µm particles, 4.06% +/- 0.64 for 3.1

286   µm beads, 2.96 +/- 0.47 for 6.8 µm beads, and 0.82% +/- 0.03 for 16.5 µm beads; Figure 1B).

287   Uptake for all sizes except the largest bead sizes (16.5 µm), was significantly higher compared

288   to the no-PS control for concentrations ≥10 ug/ml.

289   After a 3-day exposure, only the highest PS microbeads concentration (100 µg/ml)

290   showed a significant increase in APC750$^+$ cells as compared to no beads, and only when using

291   the smallest bead size (0.83 µm; Supplemental Figure 2). From these data, it follows that

292   rainbow trout myeloid lineage (Q4E$^+$) cells can take up significant amounts of PS microbeads

293   after exposure for 16 hours, and that the abundance of cells with phagocytosed beads

294   decreases significantly after this time, as was also seen for the CLC cell line. To determine

295   whether PS microbeads effected viability of phagocytic cells, we used the Live-or-Dye PE

296   assay. However, we did not detect any significant differences in cell death between samples for

297   the time periods studied.

298   To investigate effects of PS microplastics on phagocytic B cells, we used B cell marker

299   Pax5 together with the SA-APC750 reagent in a flow cytometric approach. Results showed that

300   B cells took up the smallest (0.83 µm) PS beads most efficiently, compared to the three larger

301   sizes (Figure 2A). When using 0.83 µm sized PS beads at 100 µg/ml, the average percentage

302   of APC750$^+$/Pax5$^+$ cells was 15.1% +/- 0.57 after 16 hours incubation (Figure 2A), but

303   abundance was reduced to 3.4% +/- 0.27 after 3 days (Supplemental Figure 3). This pattern of

304   reduced abundance of phagocytosis-positive B cells over time was similar to what was

305   observed for rainbow trout myeloid cells and the carp macrophage cell line.

306   B cells (Pax5$^+$) were significantly more efficient at taking up 0.83 µm beads than non-B

307   cells (Pax5$^-$ cells; Figure 2B). For 6.8 µm PS microbeads, the opposite pattern was observed;

308   more Pax5$^-$ (non-B) cells took up 6.8 µm beads compared to Pax5$^+$ cells (Figure 2B). As

309   expected, very few cells took up the 16.5 µm beads (the size of these PS microbeads is ≥ the

310   size of the average immune cell), and this pattern was similar for both Pax5$^+$ and Pax5$^-$ cells

311   (Figure 2B). No effect of microbeads on cell viability was observed for any bead size, time of

312   exposure, or concentration, using the Live-or-Dye dye (results not shown).

313   In conclusion, both myeloid and B cell populations were able to phagocytose PS

314   microbeads, with the 0.83 µm beads being more efficiently phagocytosed by B cells compared

315   to myeloid cells, and vice-versa for the 6.8 µm beads. As expected, phagocytosis by 16.5µm PS

316   beads size was very low, independent of cell type.

317

318   **Changes in abundance of immune populations after exposure to PS microbeads**

319   Next, possible changes in cellular abundance were determined for B and myeloid cells,

320   using the same markers, Q4E and Pax5. No significant changes in abundance of myeloid-

321   lineage (Q4E$^+$/Pax5$^-$) cells were detected after 16 hours or 3 days of particle exposure,

322   independent of particle size or concentration (Supplemental Figure 4). In contrast, a size- and

323   concentration-dependent decrease in B cell (Q4E$^-$/Pax5$^+$) abundance were first detected after

324   16 hours (Supplemental Figure 5) but was highly significant for all four bead sizes after 3 days

325   (Figure 3A).

326   Interestingly, a strong and dose-dependent reduction in cellular abundance was seen for

327   a subpopulation of Pax5-positive B cells that expressed Q4E (phenotype Q4E$^+$/Pax5$^+$).

328   Previously, we had suggested that this population represents a population of early developing B

329   cells (MacMurray et al., 2013; Moore et al., 2019). Using three-color flow cytometry, we

330   measured that of 10.8% +/- 0.62 cell abundance, the great majority was APC750 negative: only

331   0.62% +/- 0.14 had taken up beads after 16 hrs exposure to (100 µg/ml 0.83 µm) PS beads,

332   which is less than 6 % of the Q4E$^+$/Pax5$^+$ cells. Hence Q4E$^+$/Pax5$^+$ cells have a very limited

333   capacity to phagocytose beads. This result also supports our earlier data that phagocytic Q4E$^+$

334   cells (Figure 1B) represented myeloid cells, not developing B cells.

335   To provide further evidence that Q4E$^+$/Pax5$^+$ cells were developing B cells, we used

336   marker RAG1, which is expressed in developing B cells during immunoglobulin gene

337   rearrangement (Zwollo et al, 2010). Results showed that that majority of Q4E$^+$/Pax5$^+$ cells

338   stained positive for RAG1, confirming their developing B cell status. We focused our remaining

339   experiments on this population of developing B cells, defined as Q4E$^+$/Pax5$^+$/RAG$^+$ cells. Dose-

340   dependent inhibiting effects of PS microbeads on developing B cells were observed after 16

341   hours exposure (Supplemental Figure 6), but were stronger after 3 days, and seen for all four

342   particle sizes (Figure 3B). The reduction in developing B cell abundance was seen both in *larger*

343   particles and in *smaller* particles (Figure 3B), further supporting the thesis that this effect is likely

344   independent of phagocytosis.

345

346   **Effect of PS microplastic size on abundance of developing B cells**

347   Unexpectedly, we also observed a *particle size-dependent* reduction in the developing B

348   cell population. By comparing the change in abundance of developing B cells based on *volume*

349   of PS added for each bead size, we found a very strong correlation for the smallest beads (0.83

350   µm; R^2=0.995), with a higher volume of PS beads added correlating with lower abundance of

351   developing B cells. However, only a weak correlation was seen using the largest microbeads

352   (16.5µm, R^2= 0.245). A scatter plot of the results for all four bead sizes is shown in Figure 4 and

353   suggest that addition of the large (16.5 µm) PS beads may affect developing B cells differently

354   compared to smaller beads.

355

356   **Changes in immune populations after exposure to irregularly shaped PS microparticles.**

357   To further examine effects of PS microplastics on B cells, irregularly shaped PS

358   microparticles were generated to more closely mimic the *in vivo* situation of PS microplastics

359   present in the aqueous environment of salmonid species. As a control, we prepared a similar

360   size distribution of the PS microbeads to what we had used previously (0.1% 0.83 µm beads:

361   4% 3.1 µm beads: 28% 6.8 µm beads, and 68% 16.5 µm beads) for comparison (see

362   Supplemental Figure 1). Anterior kidney cell cultures were exposed to the two PS cocktails

363   (microparticles and microbeads) for 3 days. This exposure period was chosen based on data

364   (above) showing its strong effects on abundance of developing B cells (see Figure 3B).

365   Interestingly, similar, significant and dose-dependent decreases in developing B cells were

366   observed for both the PS microparticles and the control microbead cocktail (Figure 5A).

367   Next, we determined the strength of correlation between *volume* of added PS

368   microparticles and abundance of developing B cells, as was done for the PS microbeads.

369   Interestingly, the strength of correlation for PS microparticles ($R^2 = 0.545$) was higher than for

370   the large (16.5 µm) PS microbeads ($R^2 = 0.245$), but lower than for the small (0.83, 3.1, and 6.8

371   µm) PS microbeads ($R^2 = 0.995$-0.865), as shown in Figure 4. This is in agreement with the

372   hypothesis that larger (~16 µm) microplastic sizes may affect developing B cells differently than

373   smaller PS particles.

374   An interesting pattern of non-random distribution of particles was observed using the

375   microscope: In the *absence* of microplastics, clusters of (dividing) cells normally form in the

376   tissue culture dish, and presumably represent dividing cells (Supplemental Figure 7A).

377   Interestingly, added microplastics were found to have strongly co-localized within these cell

378   clusters, both for the 16.5 µm PS microbeads (Supplemental Figure 7B) and for the PS

379   microparticles (Supplemental Figure 7C). The co-localization pattern was visible for both 16

380   hours and 3-day incubation periods. The basis for this pattern remains unclear.

381

382   **RAG1 and Ig as markers for PS-sensitive immune cells**

383   To determine whether Ig-expressing B lineage cells were affected by the PS

384   microparticles, flow cytometry was performed using either the IgM or IgT marker, in combination

385   with RAG1. Three populations of B cells can be detected using these two markers: 1). Early

386   developing B cell populations, which express RAG1, but not yet the heavy chain for IgM (HCmu)

387   or IgT (HCtau) (phenotype mu$^-$/tau$^-$/rag1$^+$), 2). An intermediate stage of developing B cells that

388   co-express RAG1 with mu or tau (phenotypes mu$^+$/rag1$^+$ or tau$^+$/rag1$^+$), and 3). Late developing

389   B cells, which express HCmu or HCtau, but no longer express RAG1 (phenotypes mu$^+$/rag1$^-$ or

390   tau$^+$/rag1$^-$; see Table I). Results show that three RAG1-expressing populations (mu$^-$/rag1$^+$, tau$^-$

391   /rag1$^+$, and mu$^+$/rag1$^+$) had reduced cell abundance in the presence of PS microparticles, while

392   late developing B cell populations (mu$^+$/rag1$^-$ and tau$^+$/rag1$^-$) did not (Figure 5B, 5C). Further,

393   tau$^+$/rag1$^+$ cell abundance was also not significantly changed by PS microparticles (Figure 5C).

394   Together, these flow cytometric experiments show that irregularly shaped PS

395   microparticles, like PS microbeads, affected a population of Ig-negative, RAG1$^+$ B cells, while

396   late developing B cells (RAG1$^-$) of either isotype (IgM / IgT) were not affected.

397

398   **Effects of PS microparticles on cell proliferation and viability of developing B cells.**

399   Next, we determined whether or not PS microparticles affected the viability of developing

400   B cells, using the Live-or-Dye PE assay. Results showed that the percentage of dead or dying

401   RAG1$^+$ cells (prior to fixing) was not affected by the presence of PS microparticles after 3 days

402   (Figure 6A; (RAG1$^+$/PE$^+$). In contrast, the percentage of healthy, "non-dying" (RAG1$^+$/PE$^-$) cells

403   *decreased* significantly between samples not exposed to particles compared to cells exposed to

404   1 and 10 µg/ml of PS microparticles (Figure 6A). Hence, the observed reduction in abundance

405   of developing B cells in the presence of PS microparticles was not caused by increased cell

406   death.

407   Next, to determine whether PS microparticles affected the proliferation of developing B

408   cells, we used Edu/Click-iT assays to measure proliferating cells in combination with RAG1

409   expression in two-color flow cytometry, and measured effects after 3 days. No significant

410   changes in the abundance of either proliferating (RAG1$^+$/Edu$^+$) or non-proliferating (RAG1$^+$/Edu$^-$

411   ) cells were observed when comparing exposure to 0, 1, and 10 µg/ml of PS particles (results

412   not shown).

413

414   **PS-induced changes in immune gene expression.**

415   To determine if the reduced cellular abundance of developing B cells after PS exposure

416   correlated with a reduction in RAG1 gene expression, we developed a Taqman RT-qPCR

417   assay. Data show a significant reduction in expression of RAG1 after 3 days exposure to 1 or 10

418   µg/ml PS microparticles (Figure 6B).

419   Next, we measured effects of PS microparticles exposure on Ig expression, using the

420   same samples as used for RAG1 expression assays. We measured levels of membrane-bound

421   HCmu (memHCmu) and membrane-bound HCtau (memHCtau). Results showed a dose-

422   dependent decrease in expression of both targets in the presence of 1 or 10 µg/ml of PS

423   microparticles (Figure 6B). Hence the average expression of all three target genes was reduced

424   after 3 days of exposure to PS microparticles.

425

426   **DISCUSSION**

427   Here we report on the inhibiting effects of PS microplastics on the abundance of rainbow

428   trout B lineage cells in culture. Our data suggest that PS microplastics have at least two

429   different effects: efficient phagocytosis of small (0.83 µm) PS microplastics by B cells, and

430   dysregulation of B cell development independent of phagocytosis by larger (16.5 µm) PS

431   microplastics.

432

433   **Phagocytosis of microplastics.**

434   Phagocytosis occurred in both myeloid and B lymphoid cells and was dose-dependent

435   for both cell lineages. Both myeloid and B lineage cells took up the smallest beads most

436   efficiently, in agreement with earlier reports in rats and mice. Champion et al. (2008) reported on

437   the significance of particle size in phagocytosis of polymeric microspheres in rat alveolar

438   macrophages and found maximum phagocytosis for particles of 2-3 µm. The authors suggest

439   that the recognition of this size range is highly conserved, as pathogen clearance is a major

440   function of macrophages. The 2-3 µm size range optimum seems to be conserved in rainbow

441   trout, which reportedly phagocytosed 2.8 µm protein-coated particles within hours after

442   exposure, mostly though scavenger receptors on macrophages (Frøystad et al., 1998).

443   The phagocytic nature of B cells has been studied in rainbow trout, and these (B1-like) B

444   cells preferentially take up particles ≤2 µm (Li et al., 2006). Phagocytic B cells are mostly small

445   (~6 µm) cells at the *mature* B cell stage (Wu et al., 2019) supporting our conclusions that

446   *developing* B cells are not capable of phagocytosing PS microplastics. Importantly, our results

447   show that mature B cells (Q4E$^-$/Pax5$^+$) were even more efficient at taking up 0.83 µm PS beads

448   compared to myeloid cells (Q4E$^+$/Pax5$^-$) in rainbow trout. In agreement with our findings,

449   Overland et al. (2010) reported that Atlantic salmon B cells had a higher phagocytic ability for 1

450   µm latex beads compared to neutrophils in anterior kidney cultures (but not in blood).

451   The vulnerability of teleost B cells to microplastics is suggested by our findings that

452   these cells were able to phagocytose small (0.83 µm) PS microbeads with high efficiency.

453   Although we were unable to measure significant loss of cell viability within the 3-day time frame,

454   others have shown that phagocytosed PS microplastics (0.1-5 µm) increased ROS levels in

455   phagocytic cells, and size-dependent induction of apoptosis (Wu et al, 2019; Hu and Palic,

456   2020). As such, we predict that microplastics may interfere with the critical role of pathogen

457   clearance by phagocytic B cells, especially during chronic exposure *in vivo* in the aqueous

458   environment.

459

Effects of PS microplastics; IgM and IgT

460

461   Our data revealed significant dose-dependent effects on developing B cells: PS

462 microplastics reduced abundance of a population of Ig-negative, RAG1$^+$ B cells in anterior

463 kidney cultures, while gene expression analyses showed a significant reduction in expression of

464 RAG1, memHCmu, and memHCtau genes after PS exposure. Together, this suggests that the

465 generation of new IgM$^+$ and IgT$^+$ B cells in anterior kidney cultures is likely inhibited by PS. In a

466 recent study our lab showed that a line of rainbow trout that is resistant to bacterial pathogen

467 *Flavobacerium psychrophilum* (Fp) through selective genetic breeding, had higher abundance of

468 IgT$^+$ developing B cells and expressed higher levels of memHCtau (Zwollo et al, 2017), both in

469 naïve animals and after Fp challenge, compared to susceptible control animals. In a different

470 study, Marancik et al. (2015) reported that both *igm* and *igt* expression to Fp was increased

471 after Fp infection. Hence the response to this pathogen is likely dependent on the presence of

472 sufficient B cells from both classes. In light of these studies one could suggest that lower

473 production of IgT$^+$ and IgM$^+$ B cells from PS microplastics exposure might reduce the ability of

474 fish to respond adequately to pathogens such as Fp. We have recently begun exploring this

475 question of PS microplasics effects on susceptibility to Fp infection in our group.

476

How do PS microplastics affect developing B cells?

478   Cell-cell interactions are essential during the maturation stages of B cells. Although little

479 is known about how such interactions drive B cell development in teleosts, detailed information

480 is available from mouse studies. Rolink et al., (2000) developed *in vitro* co-culture systems to

481 decipher B cell differentiation in mouse bone marrow (the functional equivalent of teleost

482 anterior kidney). They demonstrated that developing B cells (progenitors and pre-BI cells) will

483 maintain long-term proliferation in culture when in the presence of Interleukin 7 (IL7)-expressing

484 stromal cells. Removal of stromal cells (and IL7) induced differentiation into immature B IgM$^+$

485 cells, with direct cell-cell contact between IL7-expressing stromal cells and IL7 receptor-positive

486   developing B cells being essential for this process (Rolink et al., 2000; Aurrand-Lions and

487   Mancini, 2018; Gauthier et al., 2002; Patton et al., 2014). Hence, prevention of these essential

488   interactions will stop cell-division, and prematurely drive differentiation towards mature B cells.

489   Similar cell-cell dependent maturation mechanisms are likely present in the anterior kidney in

490   teleost species.

491   We propose that in our experimental system, PS microplastics interfered with cell-cell

492   interactions between stromal cells and proliferating RAG1$^+$ B cells, which drove accelerated

493   differentiation towards RAG1$^-$negative, more mature B cells. This hypothesis, illustrated in

494   Figure 7, would explain the observed reduction in abundance of RAG$^+$ developing B cells in

495   microplasics-exposed cultures. It is also supported by the observed reduction in gene

496   expression for RAG1, HCmu, and HCtau, in PS-exposed cells. However, the lack of measurable

497   change in cell proliferation of developing B cells does not fit the model. It is possible that cell

498   proliferation changes occur earlier during the exposure period (we only measured changes

499   during the last 16 hours of the 3-day exposure), or that the change was too small to be

500   significant. In support of an inhibiting effect on the net-production of developing B cells (either

501   because they divide slower, or because they differentiate faster), a significant decrease in the

502   percentage of live (RAG1$^+$/PE$^-$) cells was observed after exposure to PS microparticles: it

503   suggests that fewer such cells were present under these conditions.

504   Flow cytometric analysis detected a reduced abundance of RAG1$^+$ populations (either

505   cells co-expressing HCmu, or without HCmu) after PS microplastics exposure. This suggests

506   that the observed reduction in memHCmu and memHCtau gene expression detected by qPCR

507   was caused by a reduced abundance of early developing B cells (which still express RAG1), but

508   not of late developing/immature B cells (which lack RAG1). *In vivo*, this could in turn lead to

509   fewer mature B cells capable of responding to pathogen. Hence, it can be argued that PS

510   microplastics lead to reduced numbers of mature B cells, a compressed B cell repertoire, and

511   consequently, a reduced and less diverse antibody response, and increased risk of infectious

512   disease. This is not only inferred for trout (studied here) and other teleosts, but may also be

513   translatable to human immune response, warranting further research as microplastic pollution is

514   particularly abundant in indoor air and dust (Hale et al., 2020).

515   Larger PS microbeads showed a weaker correlation between abundance of developing

516   B cells and volume of beads added, compared to smaller beads. This suggests that larger

517   particles behave differently than smaller particles in their ability to interfere with B cell

518   development. We propose that larger (>6.8 µm) microplastics are better at dysregulating B cell

519   development through interference in cell-cell interactions, compared to smaller particles, as their

520   larger size may result in greater steric hindrance (compare Figure 7B and 7C).

521   Alternatively, larger particles may be more disruptive to the organization of niche

522   structures, highly structured locations where developing B cells differentiate/reside (Tokoyoda et

523   al., 2004). The observations on the co-localization of microplastics with clusters of proliferating

524   cells supports this model, although this theory clearly requires further investigation.

525

526   **Differences between effects of microbeads versus microparticles.**

527   The results presented here expand upon previous immune work using spherical plastic

528   microbeads, by inclusion of fragments produced from actual post-consumer product PS

529   products. Although the convenience of commercially available microbeads and their ability to be

530   biotinylated for fluorescence-marker work is advantageous, their chemistries and shapes may

531   be markedly different than secondary plastics common in the environment (Rochman et al.,

532   2019). Indeed, many of the published studies cited use plastic microbeads to evaluate cellular

533   processes following exposure to pathogens and were not intended to elucidate consequences

534   of environmental microplastic pollution. The work here illustrating similar response to primary

535   microbeads and lab-generated secondary microparticles (with the exception of phagocytosis

536   work, as generated particles were not biotinylated) illustrates that conclusions from previous

537   microbead-based work may be pertinent in assessing secondary microparticle risk, at least in

538   the case of PS beads and expanded PS foam microplastics. In addition, microparticles were not

539   stored in preservatives, suggesting the effects of some preservatives in purchased microbeads

540   did not have an effect on results shown here, as illustrated by other authors (Pikuda et al.,

541   2019).

542   An unintended benefit of using PS microparticles outside of the phagocytic size range

543   was that it revealed a novel mechanism whereby larger microplastics (10-20 µm) may interfere

544   with cell-cell interactions essential for proliferation of developing B cells, potentially

545   dysregulating the B cell maturation process. Further, the technique for generating and sieving

546   plastics to reach a desirable size range (used here) should be expanded to other polymer types,

547   including polyethylene and polypropylene, which are underrepresented in immune work despite

548   their large contribution to environmental debris (Jacob et al., 2020).

549

550   **How does this extrapolate to effects of PS microplastics in vivo?**

551   In order to apply our *in vitro* data to predicting effects on *in vivo* exposure of PS

552   microplastics to hematopoietic environments, one important question concerns the possible

553   transport mechanisms of PS microplastics from mucosal areas (e.g., gills or gut) to the

554   hematopoietic site. A number of immune cells, including macrophages, neutrophils, dendritic

555   cells and B cells, are able to phagocytose small microplastics very efficiently (reviewed in

556   Gustafson et al., 2015) and there is evidence that they take up PS particles from the blood or

557   tissues. Because these cells are in the circulation, they can deliver PS microplastics to the

558   anterior kidney, which is a highly efficient site to clear particulate matter from the blood of fish

559   (Moore et al., 1998).

560   The size thresholds limiting microplastic phagocytosis need further investigation. In

561   mice, the upper particle limit for phagocytosis is surprisingly high: bone-marrow derived

562   macrophages (which measure 13.8+/-2.3 µm) could phagocytose latex beads greater than 20

563   µm, but the ingestion of beads ≥15 µm required IgG-opsonization (Cannon and Swanson,

564   1992). However, it is generally assumed that the upper threshold for phagocytosis is ≤10 µm

565   (reviewed in Gustafson et al, 2015). The latter is in agreement with our own data, which showed

566   that PS microplastics up to 6.8 µm could still be phagocytosed, although less efficiently, while

567   phagocytic B cells are highly efficient at taking up smaller particles (0.83 µm), and these

568   patterns are likely to be the same *in vivo*. It should be pointed out that although small

569   microplastics are likely the most abundant sizes, virtually all field surveys of their presence in

570   natural waters fail to measure particles < 20 µm (and often < 300 µm) due to sampling and

571   detection limitations (Hale et al., 2020).

572

573   In conclusion, in our study we provide evidence of a potentially detrimental effect of PS

574   microplastics on B cell development, using a primary cell culture system. Our data provide a

575   model to focus future *in vivo* studies on the dysregulating effects of PS microplastics on B cell

576   developmental pathways in primary immune organs of fish and humans.

577

582

583   **FIGURE LEGENDS**

584   **Figure 1.** Percentage of cells with phagocytosed PS microbeads after 16 hours of exposure.

585   Concentrations (0-100 µg/ml) for each bead size (0.83-16.5 µm) on X-axis. PS microbeads

586   0.83µm (white), 3.1µm (light grey), 6.8µm (dark grey), and 16.5µm (black), * p≤0.05, **p≤0.01,

587   ***p≤0.001. **A.** Carp macrophage cell line CLC. Average percentage of APC750^{+} cells +/−

588   standard error (n = 4) is shown in log-scale on the Y-axis. **B**. Rainbow trout anterior kidney cells.

589   Average percentage of APC750$^+$/Q4E$^+$ cells +/– standard error (n = 4) is shown in log-scale on

590   the Y-axis.

591

592   **Figure 2.** Average abundance of phagocytosis (in percentages) after 16 hours of PS-microbead

593   exposure, in rainbow trout cultures. **A.** APC750$^+$/Pax5$^+$ B cells; average +/- standard error (n=4)

594   in log-scale, on Y-axis. Concentrations (0-100 µg/ml) for each bead size (0.83-16.5 µm) on X-

595   axis. PS microbeads 0.83µm (white), 3.1µm (light grey), 6.8µm (dark grey), 16.5 µm (black), **B.**

596   APC750$^+$ cells; average +/- standard error (n=4), comparing B-cells (Pax5$^+$/APC750$^+$; dots) to

597   non-B cells (Pax5$^-$/APC750$^+$, diagonally striped), by PS particle size (in µm) on the X-axis, for

598   100 µg/ml PS beads. * p≤0.05, **p≤0.01, ***p≤0.001.

599

600   **Figure 3.** Effects of PS microbead size and concentration on cellular abundance (in

601   percentages) of two different B lineage populations after 3 days of exposure. Average +/–

602   standard error (n = 4) is shown on the Y-axis. Concentrations (0-100 µg/ml) for each bead size

603   (0.83-16.5 µm) on X-axis. PS microbeads 0.83µm (white), 3.1µm (light grey), 6.8µm (dark grey),

604   and 16.5 µm (black). * p≤0.05, **p≤0.01, ***p≤0.001. **A.** Immature/mature B cells (Q4E$^-$

605   /Pax5$^+$). **B.** Developing B cells (Q4E$^+$/Pax5$^+$/RAG1$^+$).

606

607   **Figure 4.** Correlations between the relative abundance of developing B cells and the volume of

608   PS microbeads added to the culture, comparing effects of 4 bead sizes. 3-day exposure to PS

609   beads. Relative change in abundance (in percentages) of developing B cells (Y-axis) refers to

610   each value of abundance divided by the value for "no beads". Volume of PS microbeads is

611   shown on the X-axis in units x 10^{-8} cm^3. R^2 values are shown for each correlation.

612

613   **Figure 5.** Flow cytometric analysis on effects of PS microparticles on developing B cell

614   populations. Cellular abundance (in percentage, on the Y-axis) of after 3 days of exposure.

615 Average +/- standard error. * p≤0.05, **p≤0.01, ***p≤0.001. **A.** Three-color flow cytometry to

616 detect Q4E+/Pax5+/RAG1+ cells; comparing effects of PS microbead control cocktail (left,

617 blocks) to those of PS microparticles (right, dots) for different concentrations (0-100 µg/mL, X-

618 axis). (n=6). **B** and **C**. Two-color flow cytometry; effects of PS microparticle exposure on cellular

619 abundance of early and late developing B cell populations for 0, 1, and 10 µg/ml on the X-axis.

620 (n=6). **B.** Using markers HCmu (mu) and RAG1 (rag), showing early (mu⁻/rag⁺; orange),

621 intermediate (mu⁺/rag⁺; blue), and late (mu⁺/rag⁻; grey) developing B cells of the IgM class. **C.**

622 Using HCtau (tau) and RAG1 (rag), showing early (tau⁻/rag⁺; green), intermediate (tau⁺/rag⁺;

623 red), and late (tau⁺/rag⁻; yellow) developing B cells of the IgT class.

624

625 **Figure 6.** Effects of PS microparticles on viability of developing B cells and immune gene

626 expression; 3 days of PS microparticle exposure. Average +/- standard error. * p≤0.05,

627 **p≤0.01, ***p≤0.001. (n=6). **A**. Effects on cell viability using 2-color flow cytometry. RAG1⁺/PE⁻

628 cells (live cells; blue); RAG1⁺/PE⁺ cells (dead/dying cells; orange). **B.** Relative changes in gene

629 expression of rag1, memHCmu, and memHCtau, using RT-qPCR. Target genes are shown

630 below the X-axis. PS microparticle concentrations 0 (white), 1 (grey), or 10 (black) µg/ml.

631 Relative fold-change in gene expression normalized to the "no particle" (0 µg/ml) fold-change

632 value set to 100% on the Y-axis.

633

634 **Figure 7.** Hypothesis: PS microplastics (in blue) interfere with (proliferation) signals (from IL7)

635 on stromal cells (in green) to developing B cells (in orange). The proliferation signals are

636 indicated by a yellow arrow. In the absence of this interaction, developing B cells will start to

637 differentiate towards immature B cells. The more microplastics are present in a culture, the less

638 likely it is that a stromal cell will interact with a developing B cell. Consequently, on the average,

639 developing B cells receive fewer proliferation signals, and may differentiate prematurely. **A.** In

640 the absence of PS microplastics, IL7 normally provides a proliferation signal to the pre-B cells

641 and this delays differentiation. **B.** Smaller PS microplastics interfere with the signal by blocking

642 IL7 on stromal cells. **C.** Larger PS microplastics (with *the same* total volume compared to

643 smaller particles) interfere both directly by blocking IL7 access, and indirectly through greater

644 steric hindrance.

645

646 **REFERENCES.**

647 Aurrand-Lions, M., and Mancini, S.J.C. (2018). Murine Bone Marrow Niches from

648 Hematopoietic Stem Cells to B Cells. Int. J. Mol. Sci. 19.

649 Barr, M., Mott, K., and Zwollo, P. (2011). Defining terminally differentiating B cell populations

650 in rainbow trout immune tissues using the transcription factor XbpI. Fish Shellfish Immunol.

651 31, 727–735.

652 Borrelle, S. B., Rochman, C. M., Liboiron, M., Bond, A. L., Lusher, A., Bradshaw, H., &

653 Provencher, J. F. (2017). Opinion: Why we need an international agreement on marine

654 plastic pollution. PNAS, 114(38), 9994–9997.

655 Bucci, K., Tulio, M. & Rochman, C. M. (2019). What is known and unknown about the effects

656 of plastic pollution: A meta-analysis and systematic review. Ecol. Appl. 30, 1–16.

657 Brun, NR, Koch, BEV, Varela, M., Peijnenburg WJ, Spaink, HP, and Vijver, MG. (2018).

658 Nanoparticles induce dermal and intestinal innate immune responses in zebrafish embryos.

659 Envir. Sci. Nano. 5:904-916

660 Cannon, G.J., and Swanson, J.A. (1992). The macrophage capacity for phagocytosis. J.

661 Cell Sci. 101 (Pt 4), 907–913.

662 Champion, J. A.; Walker, A.; Mitragotri, S. (2008). Role of Particle Size in Phagocytosis of

663 Polymeric Microspheres. Pharm. Res. 25 (8), 1815–1821.

664   Chappell, M.E., Epp, L., and Zwollo, P. (2017). Sockeye salmon immunoglobulin VH usage

665   and pathogen loads differ between spawning sites. Dev. Comp. Immunol. 77, 297–306.

666   Choi, J. S.; Jung, Y. J.; Hong, N. H.; Hong, S. H.; Park, J. W. (2018). Toxicological Effects of

667   Irregularly Shaped and Spherical Microplastics in a Marine Teleost, the Sheepshead

668   Minnow (Cyprinodon Variegatus). Mar. Pollut. Bull. 129 (1), 231–240.

669
670   DeLuca, D. (1983). Lymphocyte heterogeneity in the trout, Salmo gairdineri, defined with

671   monoclonal antibodies to IgM. Eur. J. Immunol. 173, 7317–7323.

672   Espinosa, C., Beltrán, J. M., Esteban, M. A., & Cuesta, A. (2018). In vitro effects of virgin

673   microplastics on fish head-kidney leucocyte activities. Environmental Pollution, 235, 30-38.

674   Frøystad, M.K., Rode, M., Berg, T., and Gjøen, T. (1998). A role for scavenger receptors in

675   phagocytosis of protein-coated particles in rainbow trout head kidney macrophages. Dev.

676   Comp. Immunol. 22, 533–549.

677   Gauthier, L., Rossi, B., Roux, F., Termine, E., and Schiff, C. (2002). Galectin-1 is a stromal

678   cell ligand of the pre-B cell receptor (BCR) implicated in synapse formation between pre-B

679   and stromal cells and in pre-BCR triggering. Proc. Natl. Acad. Sci. U. S. A. 99, 13014–

680   13019.

681   Geyer, R.; Jambeck, J. R.; Law, K. L. (2017). Production, Use, and Fate of All Plastics Ever

682   Made. Sci. Adv. 3 (7), 25–29.

683   Greven, A.-C., Merk, T., Karagöz, F., Mohr, K., Klapper, M., Jovanović, B., and Palić, D.

684   (2016). Polycarbonate and polystyrene nanoplastic particles act as stressors to the innate

685   immune system of fathead minnow (Pimephales promelas). Environ. Toxicol. Chem. 35,

686   3093–3100.

687   Gu, W., Liu, S., Chen, L., Liu, Y., Gu, C., Ren, H. Q., & Wu, B. (2020). Single-Cell RNA

688   Sequencing Reveals Size-Dependent Effects of Polystyrene Microplastics on Immune and

689   Secretory Cell Populations from Zebrafish Intestines. Environ. Sci. Technol., 54(6), 3417–

690   3427.

691   Gustafson, H., Holt-Casper, D., Grainer, D.W., and Ghandehari, H., (2015). Nanoparticle

692   uptake: the phagocyte problem. Nanotoday 10; 2015. 487-510

693   Hale, R. C.; Seeley, M. E.; Guardia, M. J. La; Mai, L.; Zeng, E. Y. (2020). A Global

694   Perspective on Microplastics. J. Geophys. Res. Ocean. 121; 1–40.

695   Hamed, M., Soliman, H. A., Osman, A. G., & Sayed, A. E. (2019). Assessment the effect of

696   exposure to microplastics in Nile Tilapia (Oreochromis niloticus) early juvenile: I. blood

697   biomarkers. Chemosphere, 228, 345-350.

698   Hansen, J.D., Landis, E.D., and Phillips, R.B. (2005). Discovery of a unique Ig heavy-chain

699   isotype (IgT) in rainbow trout: Implications for a distinctive B cell developmental pathway in

700   teleost fish. Proc. Natl. Acad. Sci. U. S. A. 102, 6919–6924.

701   Hartmann, N. B.; Hüffer, T.; Thompson, R. C.; Hassellöv, M.; Verschoor, A.; Daugaard, A.

702   E.; Rist, S.; Karlsson, T.; Brennholt, N.; Cole, M.; Herrling, M. P.; Hess, M. C.; Ivleva, N. P.;

703   Lusher, A. L.; Wagner, M. (2019). Are We Speaking the Same Language?

704   Recommendations for a Definition and Categorization Framework for Plastic Debris.

705   Environ. Sci. Technol. 53 (3), 1039–1047.

706   Hu, M. and Palic, D. (2020). Micro and nano-plastics activation of oxidative and

707   inflammatory adverse pathways. Redox Biology 37; 101620

708   Jacob, H., Besson, M., Swarzenski, P. W., Lecchini, D. & Metian, M. (2020). Effects of Virgin

709   Micro- and Nanoplastics on Fish: Trends, Meta-Analysis, and Perspectives. Environ. Sci.

710   Technol. 54, 4733–4745.

711   Jambeck, J.; Geyer, R.; Wilcox, C.; Siegler, T. R.; Perryman, M.; Andrady, A.; Narayan, R.;

712   Law, K. L. (2015). Plastic Waste Inputs from Land into the Ocean. Science 347, 3–6.

713   Kuroda, A., Okamoto, N., and Fukuda, H. (2000). Characterization of monocloanl antibodies

714   against antigens shared with neutrophils and macrophages in rainbow trout. Fish Pathol. 35,

715   205–213.

716   Li, J., Barreda, D. R., Zhang, Y., Boshra, H., Gelman, A. E., Lapatra, S., Sunyer, J. O.

717   (2006). B lymphocytes from early vertebrates have potent phagocytic and microbicidal

718   abilities. Nature Immunology, 7, 1116-1124.

719   Limonta, G., Mancia, A., Benkhalqui, A., Bertolucci, C., Abelli, L., Fossi, M.C., and Panti, C.

720   (2019). Microplastics induce transcriptional changes, immune response and behavioral

721   alterations in adult zebrafish. Sci. Rep. 9, 15775.

722   Lu, C., Kania, P. W., & Buchmann, K. (2018). Particle effects on fish gills: An immunogenetic

723   approach for rainbow trout and zebrafish. Aquaculture, 484, 98-104.

724   MacMurray, E., Barr, M., Bruce, A., Epp, L., and Zwollo, P. (2013). Alternative splicing of the

725   trout Pax5 gene and identification of novel B cell populations using Pax5 signatures. Dev.

726   Comp. Immunol. 41, 270–281.

727   Marancik, D., Gao, G., Paneru, B., Ma, H., Hernandez, A.G., Salem, M., Yao, J.,

728   Palti, Y., and Wiens, G.D. (2015). Whole-body transcriptome of selectively bred,

729   resistant-, control-, and susceptible-line rainbow trout following experimental

730   challenge with Flavobacterium psychrophilum. Front. Genet. *5*.

731

732   Moore, C., Hennessey, E., Smith, M., Epp, L., and Zwollo, P. (2019). Innate immune cell

733   signatures in a BCWD-Resistant line of rainbow trout before and after in vivo challenge with

734   Flavobacterium psychrophilum. Dev. Comp. Immunol. 90, 47–54.

735   Moore, J.D., Ototake, M., Nakanishi, T. (1998). Particulate antigen uptake during immersion

736   immunisation of fish: the effectiveness of prolonged exposure and roles of skin and gill. Fish and

737   Shellfish Immunology, 8, 393 407

738   Overland, H.S., Pettersen, E.F., Rønneseth, A., and Wergeland, H.I. (2010). Phagocytosis

739   by B-cells and neutrophils in Atlantic salmon (Salmo salar L.) and Atlantic cod (Gadus

740   morhua L.). Fish Shellfish Immunol. 28, 193–204.

741   Patton, D.T., Plumb, A.W., and Abraham, N. (2014). The survival and differentiation of pro-B

742   and pre-B cells in the bone marrow is dependent on IL-7Rα Tyr449. J. Immunol. Baltim. Md

743   1950 193, 3446–3455.

744   Perdiguero., P., Martin-Martin, A, Benedicenti, O., Diaz-Rosales, P., Morel, E., Munoz-

745   Atienza, E., Garcia-Flores, M., Simon, R., Soleto, I., Cerutti, A., and Tafalla, C. (2019).

746   Teleost IgD+/IgM– B cells mount clonally expanded and mildly mutated intestinal IgD

747   responses in the absence of lymphoid follicles. Cell. Rep. 29;4223-4235.

748

749   Pikuda, O., Xu, E. G., Berk, D. & Tufenkji, N. (2019). Toxicity Assessments of Micro- and

750   Nanoplastics Can Be Confounded by Preservatives in Commercial Formulations. Environ.

751   Sci. Technol. Lett. 6, 21–25.

752

753   Quddos, F., and Zwollo, P. (2021). A BCWD-Resistant line of rainbow trout is less sensitive

754   to cortisol implant-induced changes in IgM response as compared to a susceptible (control)

755   line. Dev. Comp. Immunol. 116, 103921.

756   Rochman, C. M. Brookson, C., Bikker, J., et al (2019). Rethinking microplastics as a diverse

757   contaminant suite. Environ. Toxicol. Chem. 38, 703–711.

758

759   Rolink, A.G., Schaniel, C., Busslinger, M., Nutt, S.L., and Melchers, F. (2000). Fidelity and

760   infidelity in commitment to B-lymphocyte lineage development. Immunol. Rev. 175, 104–

761   111.

762   Rubio, L., Barguilla, I., Domenech, J., Marcos, R., & Hernández, A. (2020). Biological

763   effects, including oxidative stress and genotoxic damage, of polystyrene nanoparticles in

764   different human hematopoietic cell lines. Journal of Hazardous Materials, 398, 122900.

765   Salinas, I., Zhang, Y.-A., and Sunyer, J.O. (2011). Mucosal immunoglobulins and B cells of

766   teleost fish. Dev. Comp. Immunol. 35, 1346–1365.

767   Seeley, M. E.; Song, B.; Passie, R.; Hale, R. C. (2020). Microplastics Affect Sediment

768   Microbial Communities and Nitrogen Cycling. Nat. Commun. 11, 1–10.

769   Tang, H., Wu, T., Zhao, Z., & Pan, X. (2008). Effects of fish protein hydrolysate on growth

770   performance and humoral immune response in large yellow croaker (Pseudosciaena crocea

771   R.). J. Zhejiang Univ. Sci. B., 9, 684-690.

772   Tokoyoda, K., Egawa, T., Sugiyama, T., Choi, B.-I., and Nagasawa, T. (2004). Cellular

773   niches controlling B lymphocyte behavior within bone marrow during development. Immunity

774   20, 707–718.

775   Veneman, W. J., Spaink, H. P., Brun, N. R., Bosker, T., & Vijver, M. G. (2017). Pathway

776   analysis of systemic transcriptome responses to injected polystyrene particles in zebrafish

777   larvae. Aquatic Toxicology, 190, 112–120.

778   Wu, L., Kong, L., Yang, Y., Bian, X., Wu, S., Li, B., Yin, X., Mu, L., Li, J., and Ye, J. (2019).

779   Effects of Cell Differentiation on the Phagocytic Activities of IgM+ B Cells in a Teleost Fish.

780   Front. Immunol. 10, 2225.

781   Xu, Z., Takizawa, F., Casadei, E., Shibasaki, Y., Ding, Y., Sauters, T.J.C., Yu, Y., Salinas, I.,

782   and Sunyer, J.O. (2020). Specialization of mucosal immunoglobulins in pathogen control

783   and microbiota homeostasis occurred early in vertebrate evolution. Sci. Immunol. 5,

784   eaay3254.

785   Yui, M. A. and Kaattari, S. L. (1987). Vibrio anguillarum antigen stimulates mitogenesis and

786   polyclonal activation of salmonid lymphocytes. Dev. Comp. Immunol. 11: 539-549.)

787   Zhang, Y. A., I. Salinas, J. Li, D. Parra, S. Bjork, Z. Xu, S. E. LaPatra, J. Bartholomew, and

788   J. O. Sunyer. (2010). IgT, a primitive immunoglobulin class specialized in mucosal immunity.

789   Nat. Immunol. 11:827-835.

790   Zitouni, N., Bousserrhine, N., Belbekhouche, S., Missawi, O., Alphonse, V., Boughatass, I.,

791   & Banni, M. (2020). First report on the presence of small microplastics (≤ 3 µm) in tissue of

792   the commercial fish Serranus scriba (Linnaeus. 1758) from Tunisian coasts and associated

793   cellular alterations. Environ. Pollution, 263, 114576.2020.

794   Zhang, N., Zhang, X.-J., Chen, D.-D., Oriol Sunyer, J., and Zhang, Y.-A. (2017). Molecular

795   characterization and expression analysis of three subclasses of IgT in rainbow trout

796   (Oncorhynchus mykiss). Dev. Comp. Immunol. 70, 94–105.

797   Zhang, Y.-A., Salinas, I., Li, J., Parra, D., Bjork, S., Xu, Z., LaPatra, S.E., Bartholomew, J.,

798   and Sunyer, J.O. (2010). IgT, a primitive immunoglobulin class specialized in mucosal

799   immunity. Nat. Immunol. 11, 827–835.

800   Zwollo, P. (2011). Dissecting teleost B cell differentiation using transcription factors. Dev.

801   Comp. Immunol. 35, 898–905.

802   Zwollo, P., Haines, A., Rosato, P., and Gumulak-Smith, J. (2008). Molecular and cellular

803   analysis of B-cell populations in the rainbow trout using Pax5 and immunoglobulin markers.

804   Dev. Comp. Immunol. 32, 1482–1496.

805   Zwollo, P., Mott, K., and Barr, M. (2010). Comparative analyses of B cell populations in trout

806   kidney and mouse bone marrow: Establishing "B cell signatures." Dev. Comp. Immunol. 34,

807   1291–1299.

808   Zwollo, P., Ray, J.C., Sestito, M., Kiernan, E., Wiens, G.D., Kaattari, S., StJacques, B., and

809   Epp, L. (2015). B cell signatures of BCWD-resistant and susceptible lines of rainbow trout: A

810   shift towards more EBF-expressing progenitors and fewer mature B cells in resistant

811   animals. Dev. Comp. Immunol. 48, 1–12.

812   Zwollo, P., Hennessey, E., Moore, C., Marancik, D.P., Wiens, G.D., and Epp, L. (2017). A

813   BCWD-resistant line of rainbow trout exhibits higher abundance of IgT+ B cells and heavy

814   chain tau transcripts compared to a susceptible line following challenge with Flavobacterium

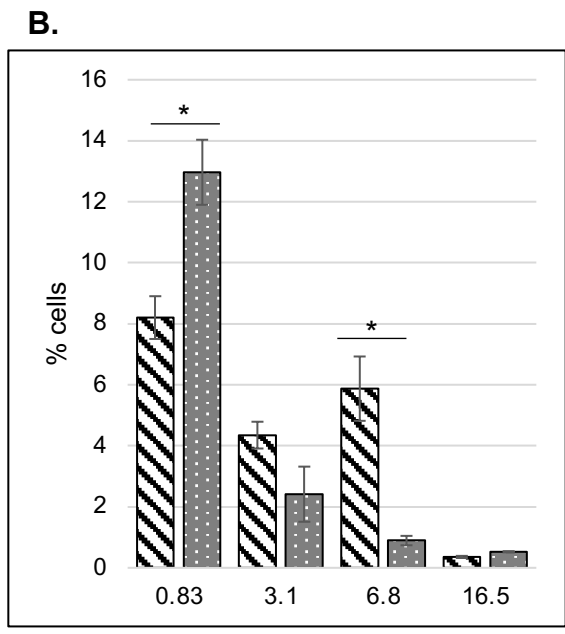815   psychrophilum. Dev. Comp. Immunol. 74, 190–199.

Figure 1.
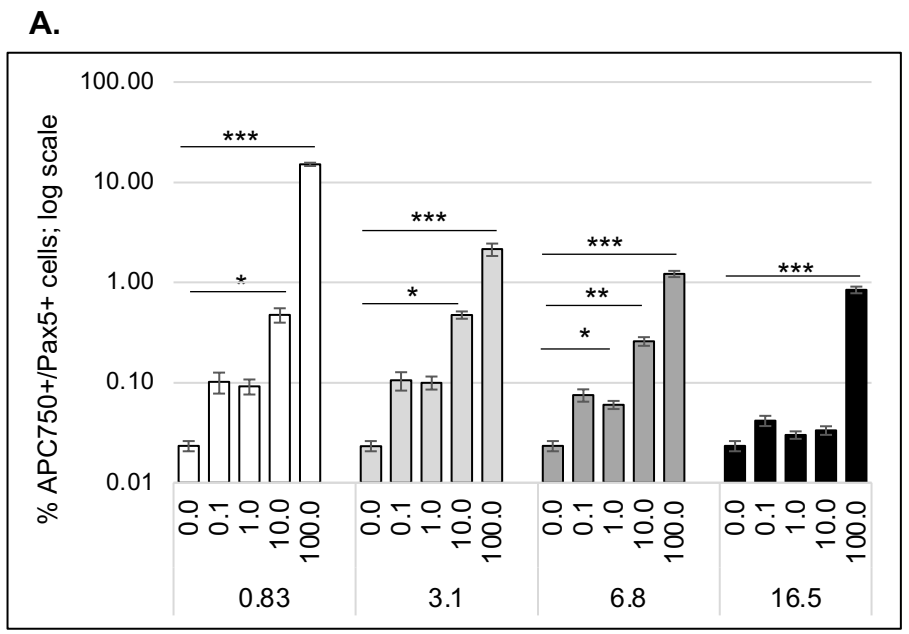
A.

B.
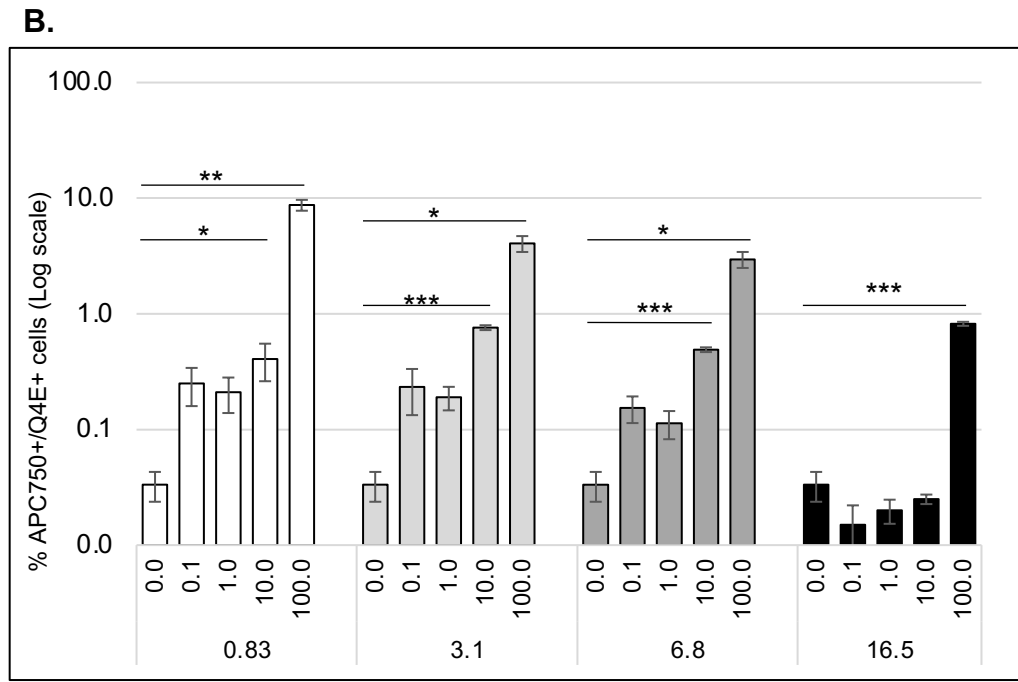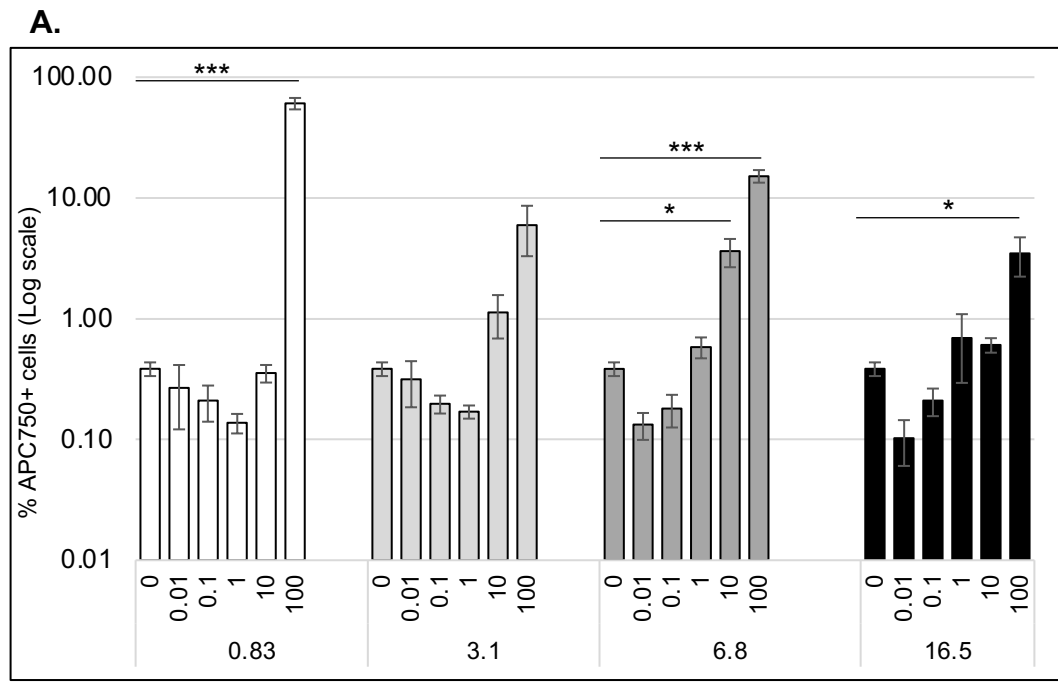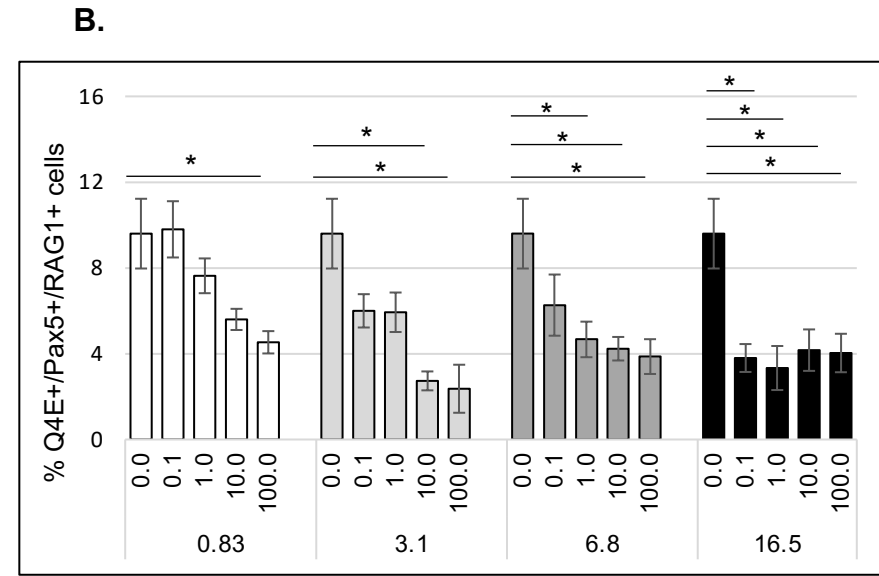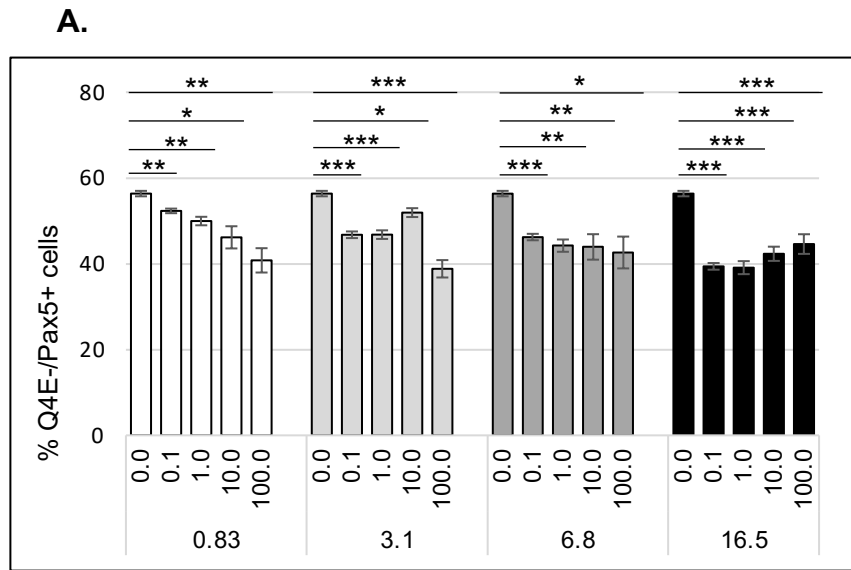
Figure 2.

Figure 3.

Figure 4

Figure 5.

A.

% cells (y-axis: 2, 6, 10, 14, 18)

PS microparticles (µg/ml) (x-axis: 0, 1, 10)

**
*

— RAG1+/PE−
— RAG1+/PE+

B.

(y-axis: 0, 20, 40, 60, 80, 100, 120)

*
**
*
*

0 1 10   0 1 10   0 1 10
RAG1   memHCtau   memHCmu
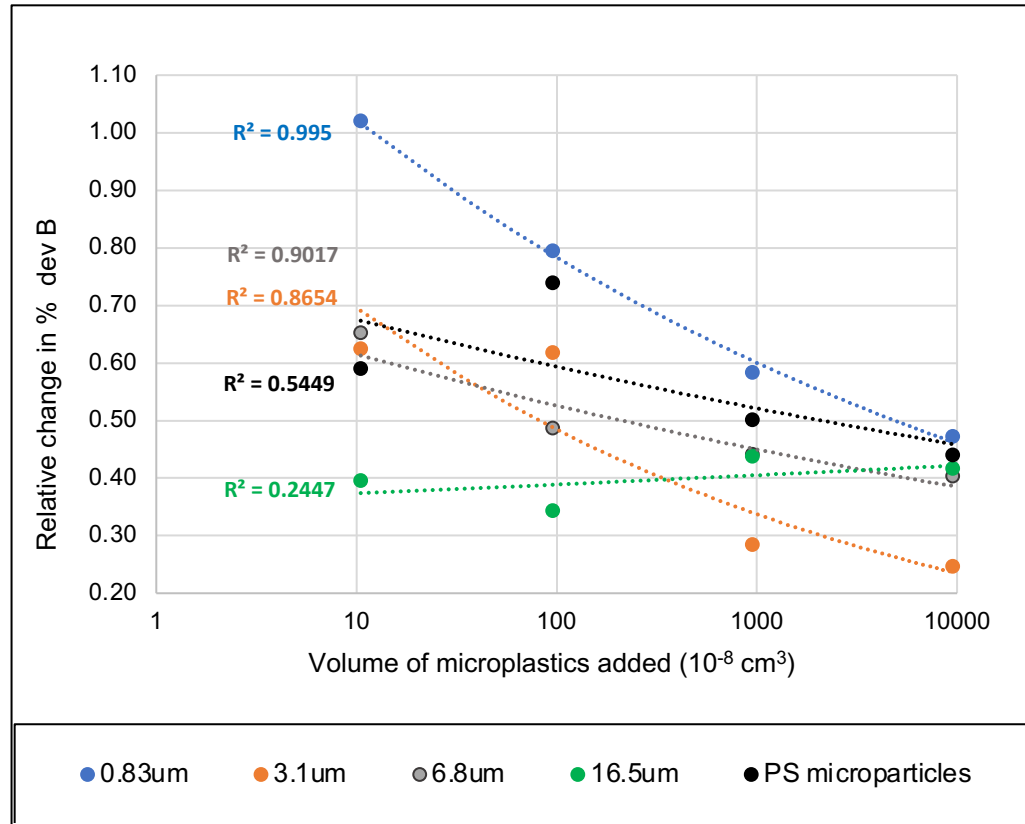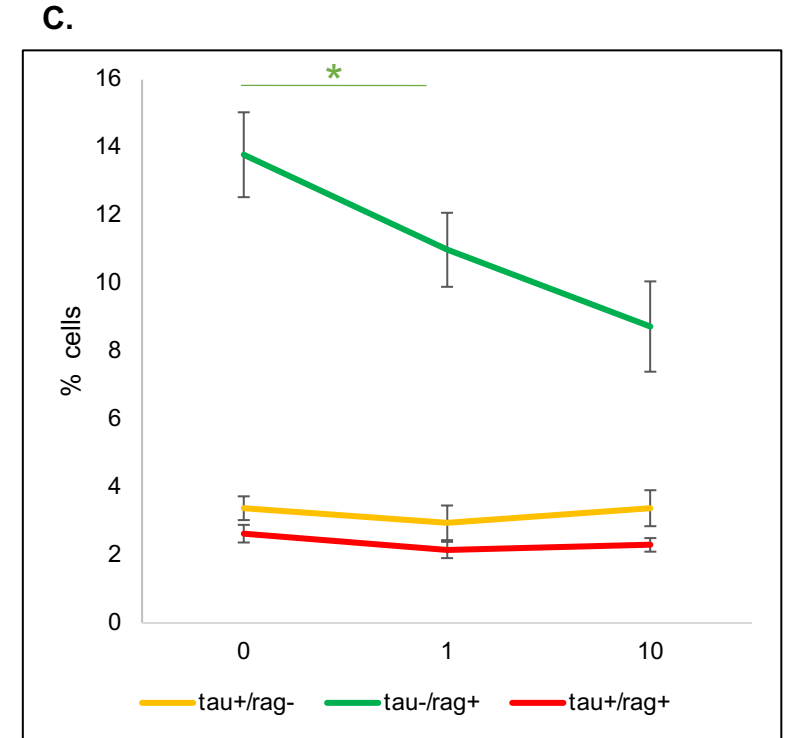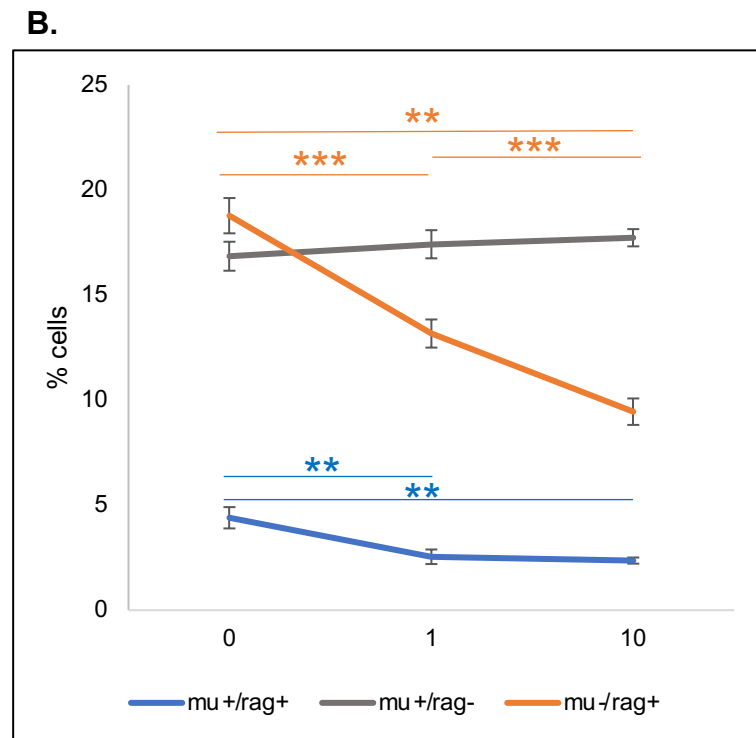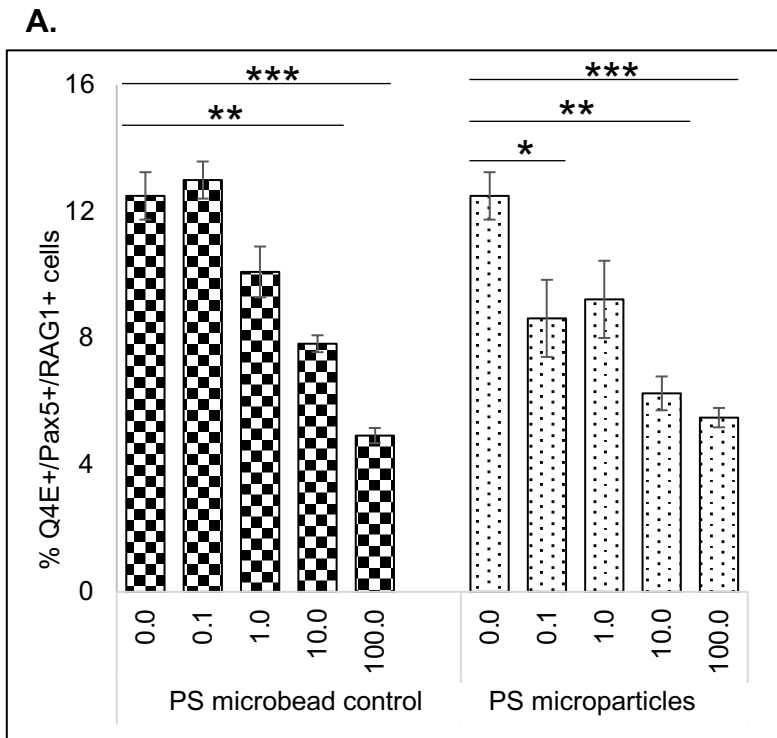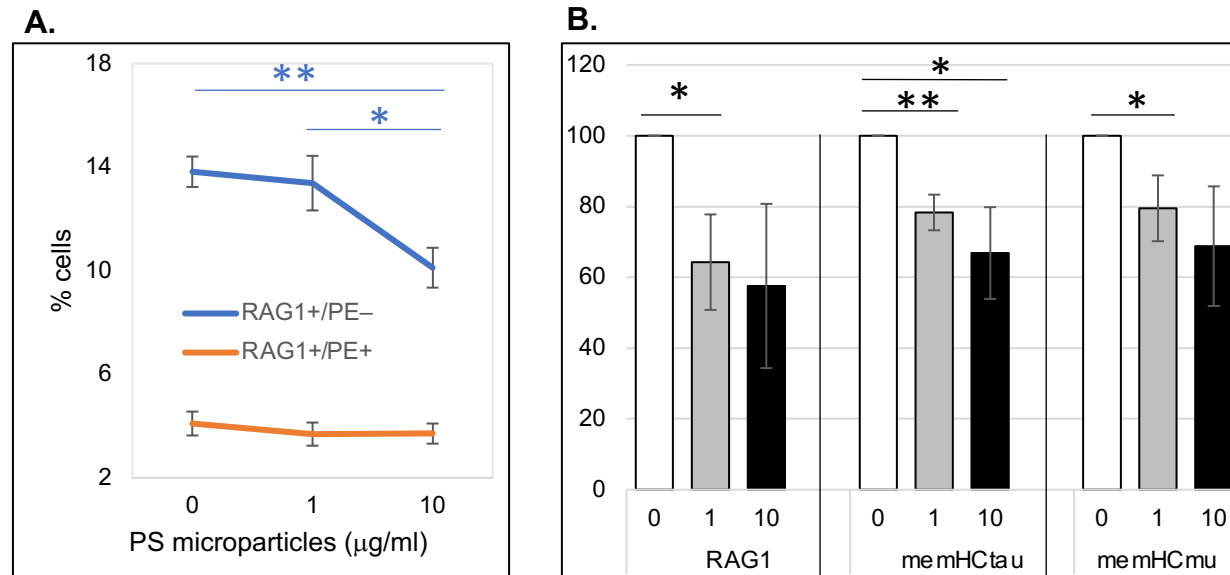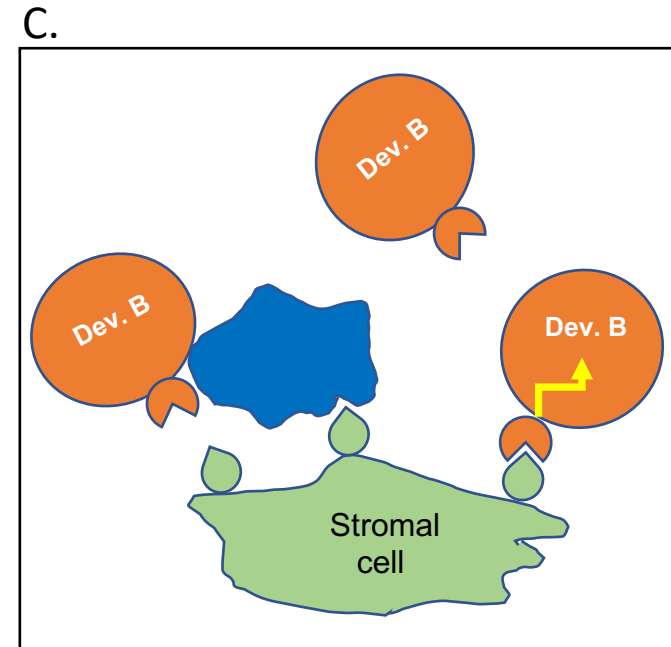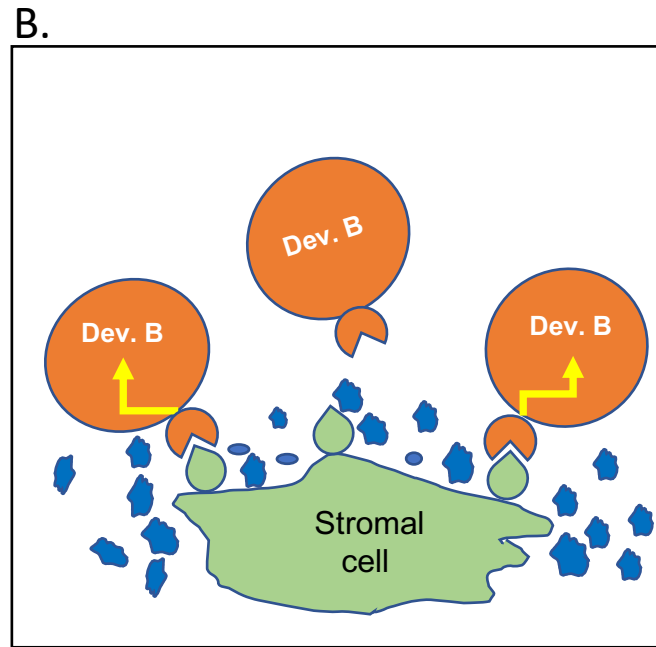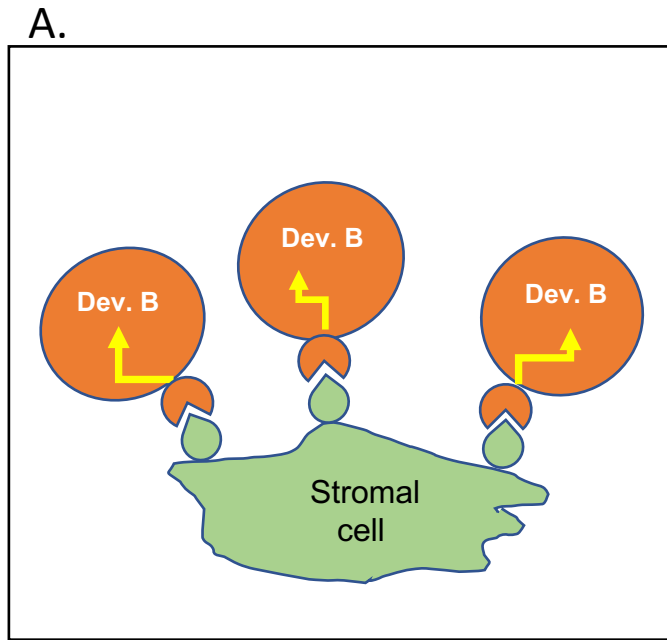
Figure 6.

Figure 7.

Cell type	Pax5	HCmu	HCtau	Q4E	RAG1
Early developing B	+	low or –	– or low	+	+
(im)mature IgM+ B	+	+	–	–	–
(im)mature IgT+ B	+	–	+	–	–
Myeloid	–	–	–	+	–

Table I. Markers used to identify B and myeloid populations in the anterior kidney